

IMECE2024-145368 DRAFT

DENSE SPRAY-COATING ACTIVE SENSING ARRAYS FOR HEALTH MONITORING OF COMPOSITE STRUCTURES

Shulong Zhou

University of Michigan-Shanghai Jiao Tong
University Joint Institute, Shanghai Jiao Tong
University, Shanghai, China

Chunquan Wang

Wuxi city huifeng electronic co. Ltd, Jiangsu, China

Yanfeng Shen

University of Michigan-Shanghai Jiao Tong
University Joint Institute, Shanghai Jiao Tong
University, Shanghai, China

Yuan Tian

Wuxi city huifeng electronic co. Ltd, Jiangsu, China

ABSTRACT

This paper proposes a dense spray-coating active sensing arrays for composite structural health monitoring via the guided wave generation and reception. The actuation-sensing capability is realized by integrating piezoelectric nano-powder into a hosting matrix, followed by the formation of an active material layer on the composite surface through a spraying process. The selective actuation and sensing of a certain guided wave mode can be achieved through the optimization of electrode configuration, in conjunction with dispersion effect. This research initiates with the analysis of the dispersion curves of composites so as to determine electrode parameters. Subsequently, three-dimensional numerical models in several array patterns, such as inter-digital (IDT) type, comb types and irregular annular array, are meticulously constructed. Single-mode generation at one direction is achieved through the meticulous design of the spatial distribution of array electrodes coupled with wavelength modulations in IDT array and comb array. At the same time, omnidirectional single-mode generation of irregular annular array is conducted through the electrode spatial distribution coupled with all direction wavelength modulations. Ultimately, the electrode configurations are numerically investigated through exciting an anti-symmetric and a symmetric type guided wave mode in a multilayer composite plate. The numerical simulation shows that the proposed spray-coating sensing arrays system possesses great potential for future composite damage detection applications. The paper finishes with summary, concluding remarks, and suggestions for future work

Keywords: spray-coating active sensing arrays; composite structures; guided waves, wave mode control

1. INTRODUCTION

Composite materials have been escalated utilization in the fabrication of aerospace components [1, 2], wind turbines [3-6], and marine equipment due to their remarkable stiffness-to-weight ratio, exceptional strength, corrosion resistance, reduced weight, and enhanced mechanical properties [7, 8]. These materials are steadily emerging as substitutes for metallic counterparts, finding widespread application across various sectors such as the fabrication of chemical containers, pressure vessels, machine spindles, power transmission shafts, and robot arms [9]. Despite the burgeoning popularity, composites present complexities in manufacturing, and detecting damage for these materials proves the challenging. Defect detection assumes a pivotal role in assessing the longevity and dependability of composite materials. Various researchers have explored techniques to discern internal damage in composite structures, including methods such as X-ray analysis [10, 11] optical testing [12-14], magnetic particles [15], infrared thermography [16, 17], and ultrasonic testing [18-20]. Of these methodologies, ultrasonic guided wave technology stands out for its exceptional reliability in evaluating the structural integrity and safety performance of composite materials [21]. Its capability to scan the cross-sectional area of a structure renders advantageous for detecting damage in advanced composite materials [22, 23].

Detecting and evaluating the structural integrity of composite materials via ultrasonic guided waves proves challenging due to the multilayered structures with anisotropic velocity distributions [24]. Moreover, damage manifested at various locations across different components, leading to complex acoustic wave propagation mechanisms. This complexity complicates the tracking of all damaged parts [25]. Therefore, selecting a sensitive and single wave mode ultrasonic

guided waves becomes essential for composite structural damage identification.

Lead zirconate titanate wafers (PZTs) [26, 27] and macro-fiber composites (MFCs) [28] are commonly used for the damage detection, adhesive bonded on the surface of the structures. Giurgiutiu et al. have conducted comprehensive research on the coupling mechanism of PZTs and mode tuning by dimensions and bonding quality through both theoretical and experimental studies [29]. Multiple PZTs were arranged in either a comb or inter-digital shape, enabling mode control through phase matching by adjusting the pitch or time delay [30-32]. Mańka et al. have developed an interdigital transducer (IDT) comprising a series of densely distributed discrete electrode strips to achieve directional narrowband wave generation [28]. However, the fragility and limited lifespan of piezoceramic-based transducers render them susceptible to failure in applications. Moreover, mode control through array transducers presents several drawbacks, impeding the practicality.

On the other hand, flexible piezopolymer-based transducers have non-brittle for offering versatility and could be effectively applied on curved structures [33]. Polyvinylidene fluoride (PVDF) stands out as the most extensively researched piezopolymer for Structural Health Monitoring (SHM) applications [34-37]. Conventional PVDF transducers typically take the form of standalone thin films or membranes. Before the installation via adhesive bonding onto structures, there are various necessary functionalization procedures such as phase transformation and polarization. However, these processes are intricate and demand meticulous control and monitoring, significantly escalating costs. Additionally, the inherently low piezoelectric constants and compliant nature of PVDF pose challenges in generating large amplitude guided waves. Therefore, the exploration of novel dense spray-coating sensing arrays which improve actuation and sensing capabilities and cost-effectiveness, holding promise for enhancing SHM performance in composite structures.

This paper proposes the utilization of dense spray-coating active sensing arrays for composite structural health monitoring via guided wave generation and reception. The actuation-sensing capability is achieved by integrating piezoelectric nano-powder into an epoxy matrix, followed by applying an active material layer onto the composite surface through a spraying process. The research commences with an analysis of dispersion curves of composites to determine electrode parameters. Subsequently, meticulous construction of three-dimensional numerical models is utilized for several array patterns, including inter-digital (IDT) type, comb types, and irregular annular arrays. Single-mode generation in a specific direction is accomplished through the careful design of array electrode spatial distribution coupled with wavelength modulations in IDT array and comb array configurations. Meanwhile, omnidirectional single-mode generation in irregular annular arrays is achieved through electrode spatial distribution combined with wavelength modulations in all directions. Finally, the electrode configurations are numerically investigated by exciting both

anti-symmetric and symmetric guided wave modes in a multilayer composite plate.

2. SPRAY-COATING ACTIVE SENSING ARRAYS DESIGN

This section provides the arrays design procedure, including the mode selection, the optimization of electrode configuration and the coating construction. Single-mode generation is achieved through the meticulous design of the spatial distribution of array electrodes coupled with wavelength modulations.

2.1 Mode selection

The selection of guided wave modes for inspection is influenced by various factors, including dispersion, attenuation, and surface displacement [38]. In this research, the plies of the plate were oriented [0, 90, 0, 90, 90, 0, 90, 0], with each layer being 0.15mm thick as depicted in FIGURE 1. The SAFE dispersion analysis software was employed to generate dispersion curves of Lamb modes [39]. FIGURE 2 illustrates the phase velocity and group velocity dispersion curves for a 1.2 mm thick CFRP composite plate in 0 direction. The array coating could be tailored to excite a specific wavelength in the plate.

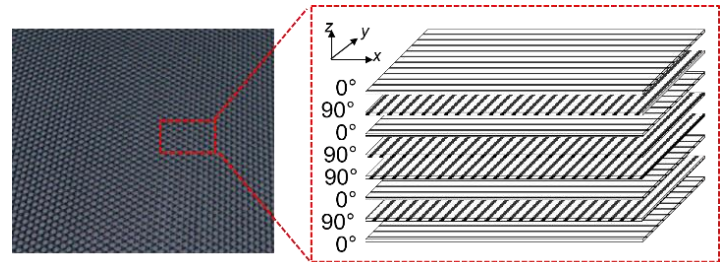


FIGURE 1: THE CARBON FIBER ORIENTATION

In a typical plate like structure infinite number of mode and frequency points exists with each having its own unique characteristics. For the analytical analysis, the wavelength, λ , of any wave mode is given by,

$$\lambda = \frac{c_p}{f} \quad (1)$$

where c_p is the phase velocity of the mode and f is the frequency. Equation (1) may also be written

$$\frac{\lambda}{d} = \frac{c_p}{fd} \quad (2)$$

where d is the plate thickness. Hence, for a specified plate thickness, these lines were represented a constant wavelength, intersecting with the dispersion curves of different modes, and the modes could be excited using a transducer tailored for this wavelength. A wavelength of 16 mm is seen intersecting several guided wave modes in FIGURE 2. In the composite plate, the S0

mode was exhibited the phenomenon with a phase velocity of 4889.6 m/s at 305.6 kHz and an A0 mode with a phase velocity of 684.8 m/s at 43 kHz. The two modes exhibit distinct surface displacement profiles, as illustrated in FIGURE 3, with the A0 mode displaying significant out-of-plane displacement and the S0 mode showing notable in-plane displacement. These differing characteristics could be exploited for condition monitoring applications. The penetration power of A0 mode was constrained by its leakage into structures, whereas the S0 mode boasted significantly higher penetration power with less leakage.

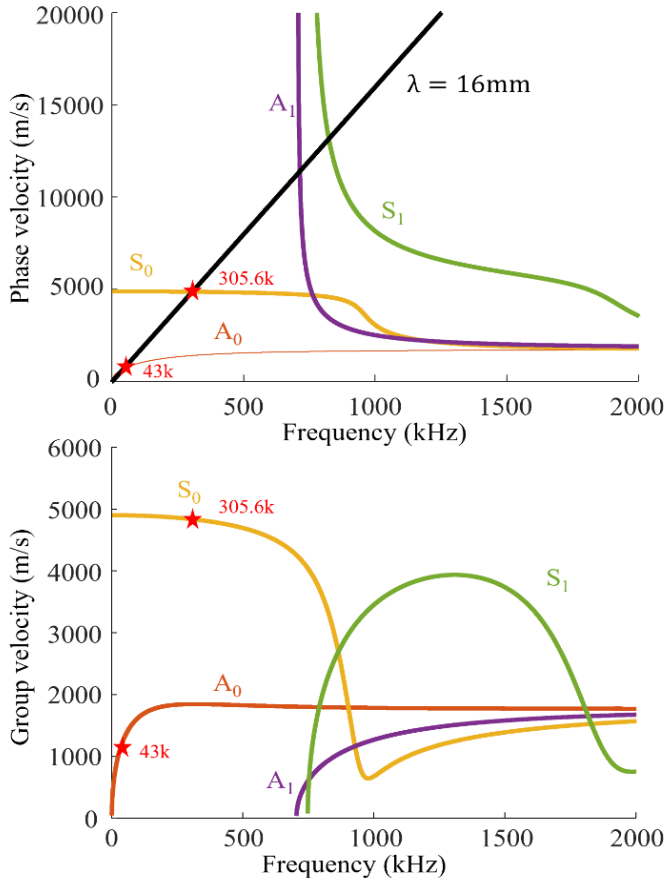


FIGURE 2: DISPERSION CURVES OF A 1.2 MM THICK CFRP PLATE SHOWING A WAVELENGTH 16 MM INTERSECTING SEVERAL MODES WITH THE S0 AND A0 MODE BEING MARKED. (A) PHASE VELOCITY; (B) GROUP VELOCITY

2.2 Design of electrode configuration

The design of the electrode configuration was inspired by the annular array transducers [40] and interdigital transducer [41] [42]. By exciting all the elements with the same amplitude, guided wave mode control was achieved by adjusting the spacing between the elements. Two distinct array patterns were investigated, namely the comb and interdigital (IDT) types, as depicted in FIGURE 4. For the comb type electrode array, voltage was applied on the same side of the adjacent electrode. Whereas for the IDT type array, voltage was applied on adjacent electrodes in the form of voltage difference.

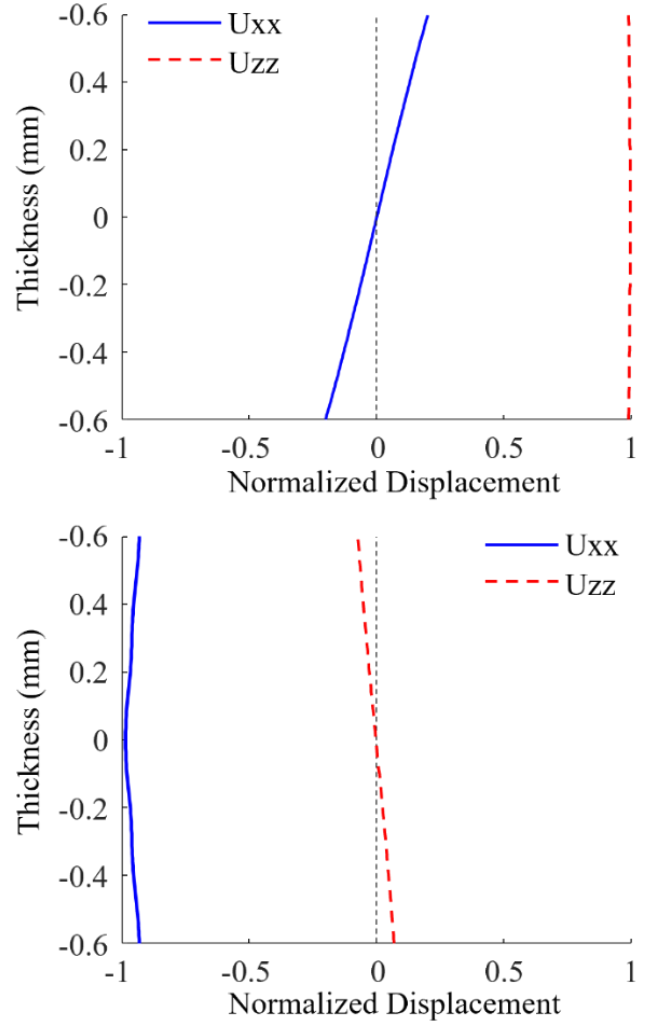


FIGURE 3: WAVE STRUCTURES ACROSS THE CROSS SECTION OF AN 1.2 MM THICK CFRP PLATE. (A) A0 MODE AT 43 KHZ; (B) S0 MODE AT 305.6 KHZ

The annular elements were assumed to have a width d , the separation between the center of the elements was a for the comb type array and $a/2$ for the IDT type array. For the comb and IDT transducer configurations, the parameters to optimize the array factor were as given in equations (3) and (4) respectively [40]

$$a \approx \lambda, \quad d = \lambda/2 \quad (3)$$

$$a \approx \lambda, \quad 0 < d < \lambda/2 \quad (4)$$

Here λ was the wavelength, The element widths used in the design were $\lambda/2$ and $\lambda/4$ for comb and IDT configurations respectively.

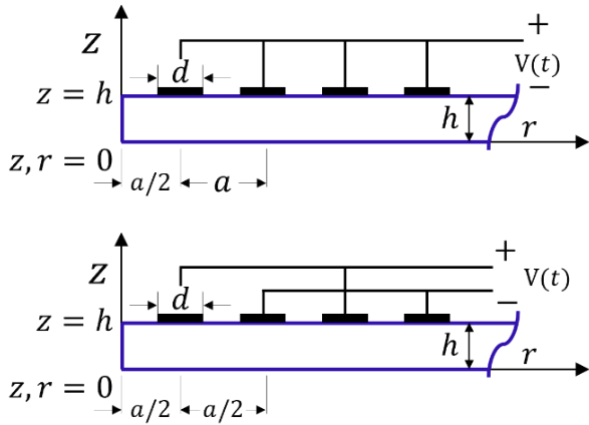


FIGURE 4: AXI-SYMMETRIC REPRESENTATION OF THE ARRAY TRANSDUCER ON PLATE. (A) COMB TYPE CONFIGURATION; (B) IDT TYPE CONFIGURATION

2.3 Coating construction

The customized piezoelectric dense spray-coating active sensing array was characterized by the absence of intricate assembly processes, without involving sintering under high-

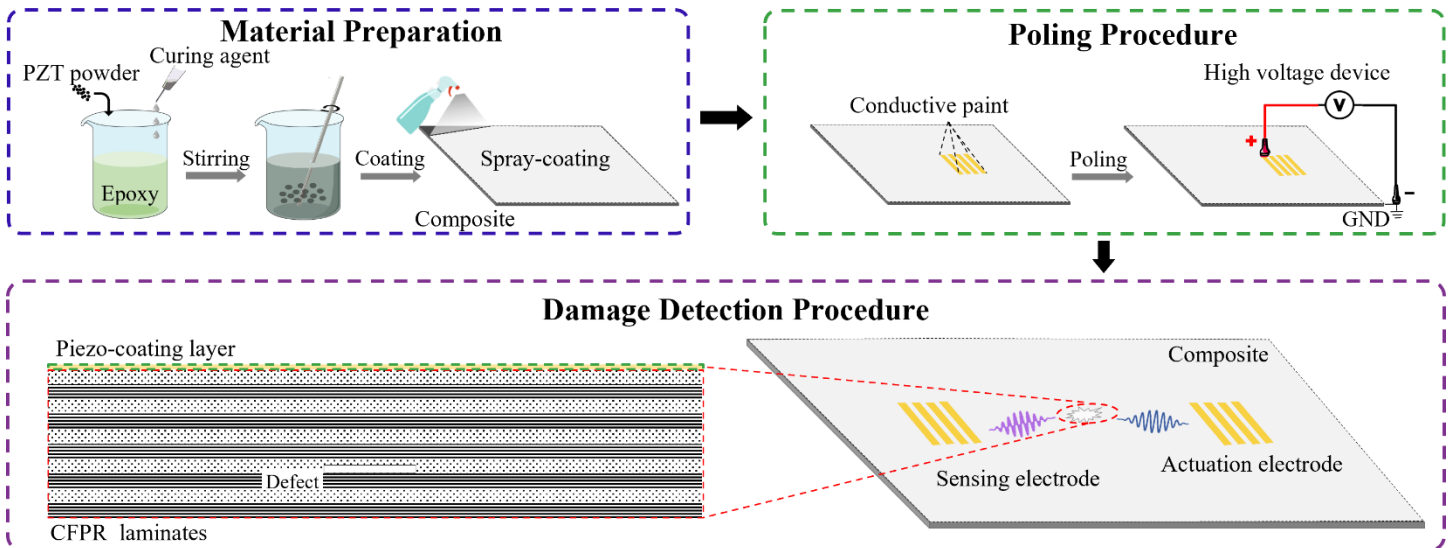


FIGURE 5: SCHEMATIC DIAGRAM FOR THE FABRICATION OF THE DENSE SPRAY-COATING ACTIVE SENSING ARRAY AND THE PROCEDURE OF DAMAGE DETECTION

3. FINITE ELEMENT MODELING

In this study, a comprehensive three-dimensional finite element (FE) model was developed using COMSOL Multiphysics. The FE model was integrated structural mechanics and electrostatics to evaluate the directional actuation efficacy of the piezoelectric dense spray-coating active sensing array. Combining the comb and IDT type sensing patterns, the generation and reception characteristics for ultrasonic wave active sensing was investigated. Furthermore, the omnidirectional irregular annular array model was employed to

temperature environments during fabrication compared with piezoelectric ceramics. The fabrication method entailed blending PZT powder and epoxy resin at a weight ratio of 5:1, with the epoxy resin composed of resin (HF-005) and hardener (HF-006) sourced from Wuxi City Huifeng Electronic Co., Ltd. A meticulous preparation protocol was involved ultrasonication to ensure thorough dispersion, followed by even spraying onto the composite surface using vacuum-based equipment. Curing proceeds was accomplished at a constant 60 degrees Celsius for 4 hours. To polarize the piezoelectric active sensing array, the electrodes was undergone silver screen printing at room temperature for 45 minutes. Poling was executed using a high-voltage amplifier submerged in air, applying 30 kV for 5 cycles. The manufacturing flow is illustrated in FIGURE 5, showcasing the versatility of designing various electrode shapes at any position on the coating surface to achieve desired actuation and sensing effects. These piezopolymer coatings exhibited exceptional performance as a novel sensing network configuration, characterized by the lightweight, ultrathin, flexible, rapid-prototyping, and adhesive-free attributes, ensuring high adaptability and consistency.

validate the capacity for single-mode guided wave generation on the composite in all directions.

3.1 Numerical simulation of the comb/IDT type arrays

In this scenario, a 280 mm × 280 mm CFRP composite plate with a thickness of 1.2 mm was served as the propagation medium. The entire surface of the CFRP plate was then modeled with a dense spray-coating active layer comprising piezoelectric materials, measuring 0.15 mm in thickness. Sensing array patterns were subsequently implemented on the coating layer,

meticulously designed through standard tuning by wavelengths $\lambda = 16\text{mm}$.

As depicted in FIGURE 6 and FIGURE 7, the sensing patterns were intricately printed on the top and bottom surfaces of the piezoelectric material, serving as the electrodes, and meticulously coated onto the CFRP plate. Each configuration exhibited unique surface displacement patterns on the piezoelectric material, directly impacting the generation of guided wave modes. The polarization direction for the piezoelectric element was assumed to be in the z-direction. Mechanical damping within the piezoelectric material was simulated using an Isotropic Loss Factor with a value of $\eta_s = 0.006$, considering a Mechanical Quality Factor (Q_m) of 80.

Employing the Equivalent Average Parameter (EAP) method, overall and nominal quantities of the piezoelectric material were utilized to mimic the coating materials property. Perfectly Matched Layer (PML) conditions were applied at the four plate boundaries to prevent wave boundary reflections. As for the boundary conditions of the electrodes, the bottom surface of the piezoelectric layer was grounded, while an electric potential boundary condition was applied to the top part. Zero charge boundary conditions were applied to the remainder of the piezoelectric element. The displacement information from the sensing points on the upper and lower surfaces of the composite plates was obtained for the mode analysis.

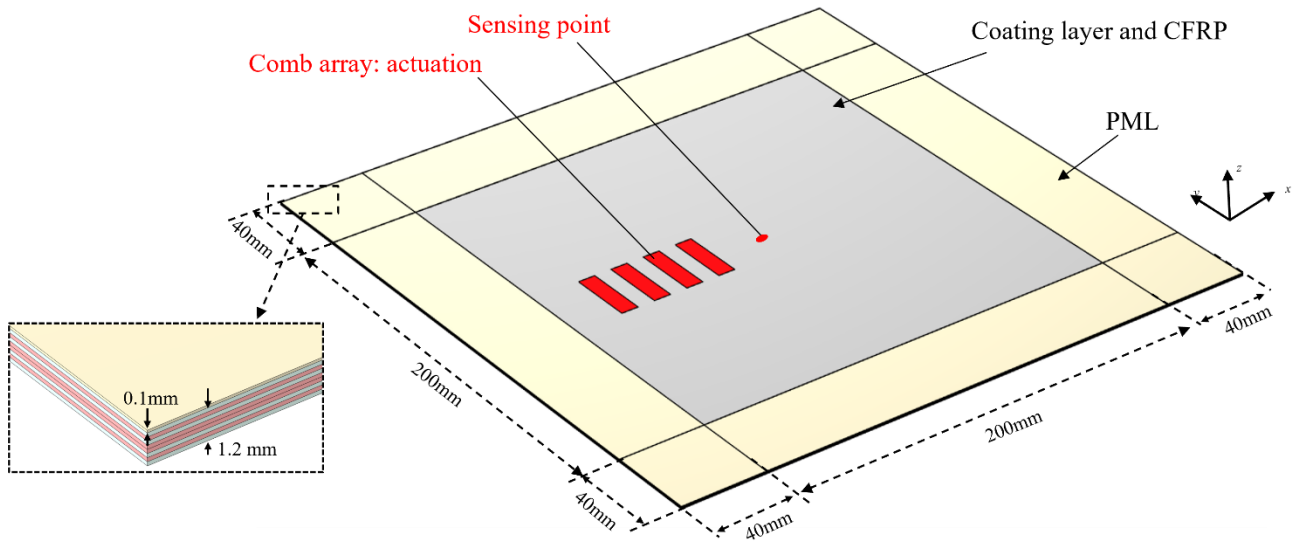


FIGURE 6: THE 3D MODEL GEOMETRY OF THE COMB TYPE SENSING

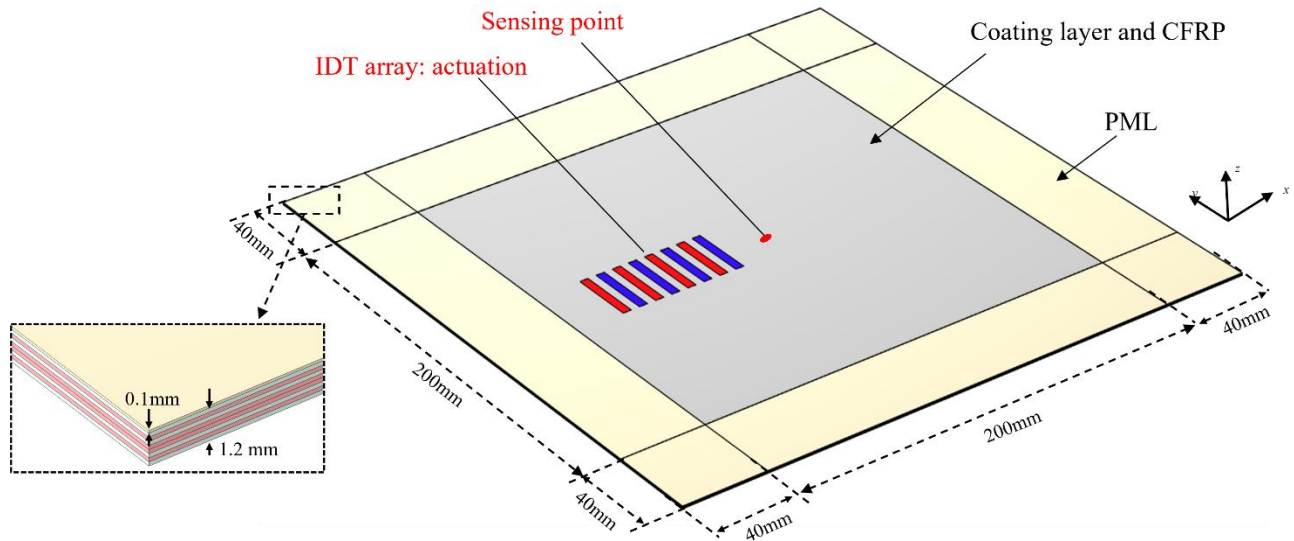


FIGURE 7: THE 3D MODEL GEOMETRY OF THE IDT TYPE SENSING

In the numerical meshing process, Free triangular elements were employed to mesh the piezoelectric layer domains, while free quad elements were used for the CFRP plate. To streamline computational complexity, a swept mesh in the z-direction was implemented for the CFRP, with a mesh size set at 10 times the shortest possible wavelength of the A0 mode. It's worth noting that the PML domains were meshed using swept mesh elements

with increasing mesh size at a low growth rate of 1.2, ensuring satisfactory mesh element quality. Simulation utilized Hanning windowed tone burst signals with 5 cycles and 100 V amplitude to excite the actuation electrode, with 43 kHz corresponding to A0 mode excitation and 305.8 kHz corresponding to S0 mode excitation.

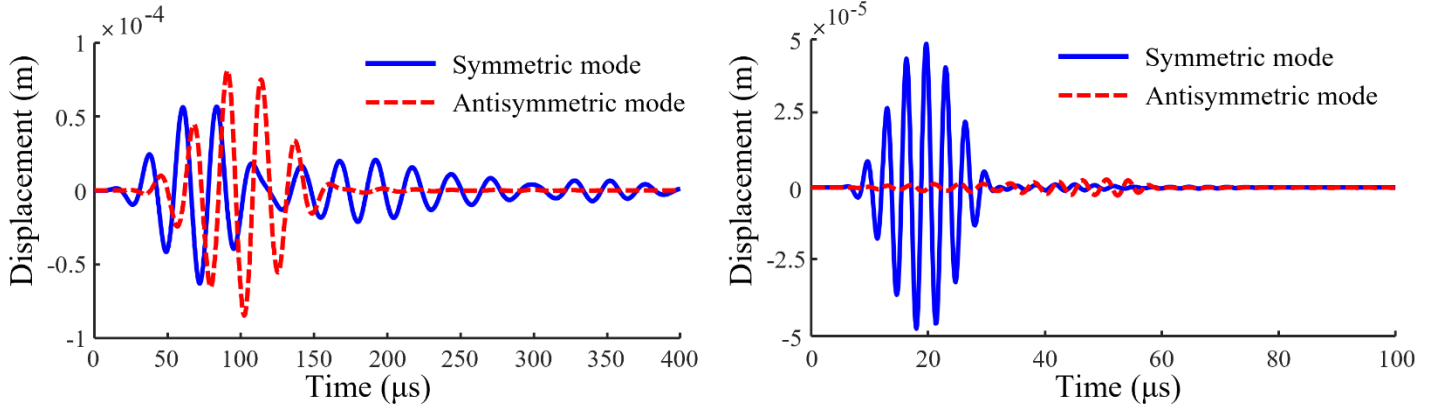


FIGURE 8: MODE ANALYSIS BY THE COMB TYPE SENSING ARRAY. (A) 43KHZ; (B) 305.8KHZ

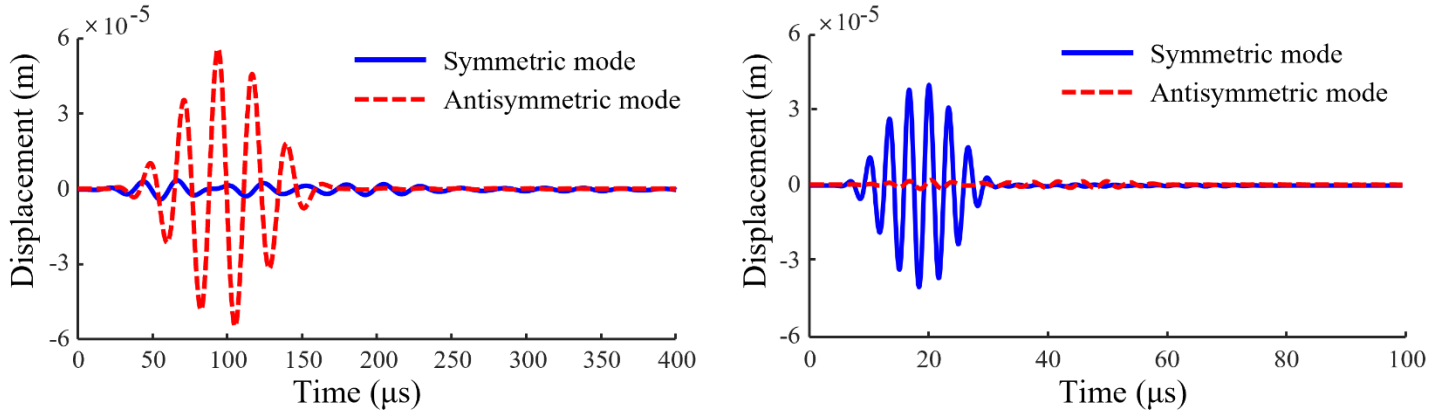


FIGURE 9: MODE ANALYSIS BY THE IDT TYPE SENSING ARRAY. (A) 43KHZ; (B) 305.8KHZ

The surface displacement on the CFRP plane for both configurations was recorded to analyze the modes. FIGURE 8 displays the A0 and S0 modes during excitation for the comb pattern model, while FIGURE 9 depicts the results from the IDT pattern model. Comparing the single-mode generation capability of the two configurations, it was evident that both excel in S0 wave generation. However, the comb type electrode efficiently excited only the S0 mode, with a larger S0 wave appearing in the A0 mode generation. Notably, the A0 mode was significantly higher in the comb type excitation compared to the IDT type. This disparity was arisen from the polarization direction of the piezoelectric material and the applied electric field, resulting in higher surface displacement for the comb type electrode model. The predominant out-of-plane loading in the comb configuration was poorly coupled to modes with significant in-plane

displacement at certain frequencies. Considering all aspects, the IDT type was emerged as the optimal electrode pattern for single-mode excitation.

3.2 Numerical simulation of the annular arrays

Understanding the dispersion characteristics of Lamb waves in multilayered media was crucial for developing guided wave-based damage detection techniques. Previous studies have primarily focused on unidirectional guided wave excitation of composites. However, dispersion curves vary in different directions owe to material anisotropy. To achieve full-field single-mode guided wave excitation in composite plates, comprehensive modulation of the annular wave field is necessary.

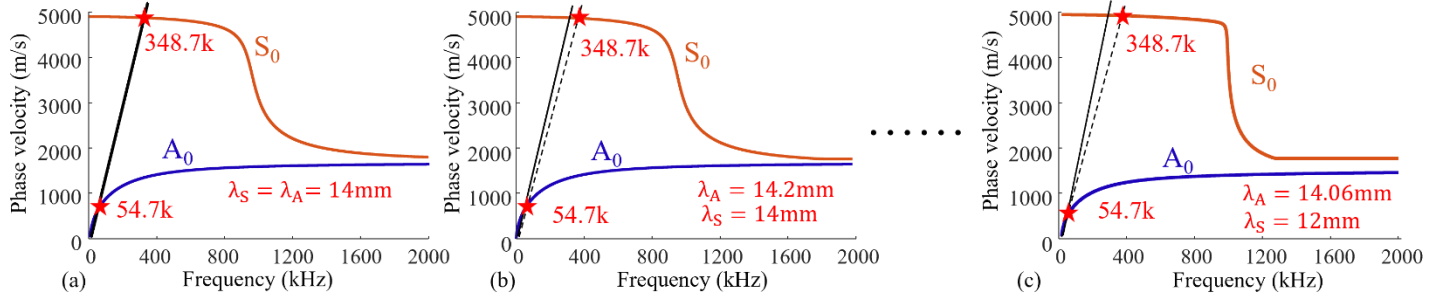


FIGURE 10: THE DISPERSION CURVE FOR A 1.2MM THICKNESS CROSS-PLY [0, 90, 0, 90, 90, 0, 90, 0] COMPOSITE AT DIFFERENT DEGREE. (A) 0 DEGREE (BASELINE); (B) 5 DEGREES; (C) 90 DEGREES

FIGURE 10 depicts the dispersion curve of the CFRP composite for the pattern parameter design of the annular array. Considering the subsequent simulation and sample production, the initial baseline wavelength was set to 14mm at 0 degrees. Notably, the wavelengths corresponding to guided waves in symmetrical and antisymmetric modes were different across all directions. For instance, while the A0 wavelength was measured as 14.06mm, the S0 wave as 12mm at 90 degrees.

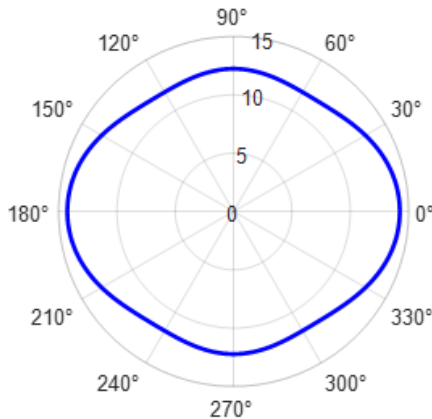


FIGURE 11: WAVELENGTH CORRESPONDING TO THE A0 MODE AT ALL DIRECTION

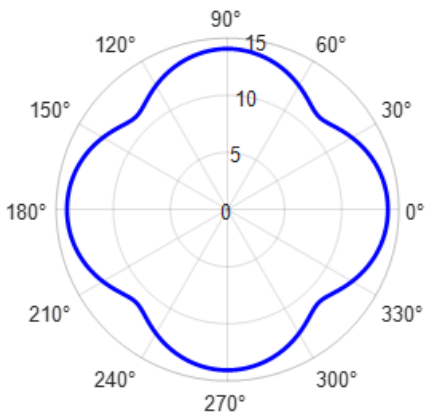


FIGURE 12: WAVELENGTH CORRESPONDING TO THE S0 MODE AT ALL DIRECTION

The wavelengths corresponding to the S0/A0 mode across all directions are illustrated in FIGURE 11 and FIGURE 12. As confirmed in FIGURE 10, for A0 mode excitation, the wavelength was decreased from 0 to 90 degrees, whereas for S0 mode, the wavelength was decreased initially and then increased.

FIGURE 13 showcases the optimized finite element model established using COMSOL Multiphysics for the single mode generation. The omnidirectional irregular annular arrays, fabricated and deployed on the CFRP plate, were utilized to excite and receive single-mode ultrasonic guided wave signals at 54.7 kHz (A0 mode) and 348.7 kHz (S0 mode). The array was comprised 8 elements, and the overall size of the plate was measured about 360 mm × 360 mm × 1.2 mm. Hanning windowed tone burst signals with 5 cycles and 100 V amplitude were employed to excite the actuation electrode. Surface displacements of the top and bottom surface in the plate were recorded at a distance of 100 mm from the axis of symmetry. For the numerical meshing procedure, the piezoelectric layer domains were meshed with free triangular elements, while free quad elements were utilized for the CFRP plate. To reduce computational complexity, a swept mesh in the z-direction was employed for the CFRP. The mesh size was determined to be 10 times the shortest possible wavelength of the A0 mode. The finite element model was contained 5,879,852 degrees of freedom, with an average element quality of 0.8.

FIGURE 14 illustrates the simulated displacement diagram on the top surface of the CFRP plate. It was evident that the displacement distribution was appeared non-uniform after the guided wave generated. This phenomenon was arisen that the wave shape was coupled with the electrode patten. Meanwhile, it was apparent that the length of the guided wave closely matches the size of the designed electrode when single modes of guided waves were excited. Regardless of the excitation mode used, the single-mode excitation effect is apparent as illustrated in FIGURE 15. However, it was evident that under pure A0 excitation, the generation of S0 mode was minimal, whereas under pure S0 mode excitation, numerous A0 mode waves were still emerged. This discrepancy was might stemmed from the accuracy of dispersion curve calculations in all directions of the composite, influencing wavelength selection.

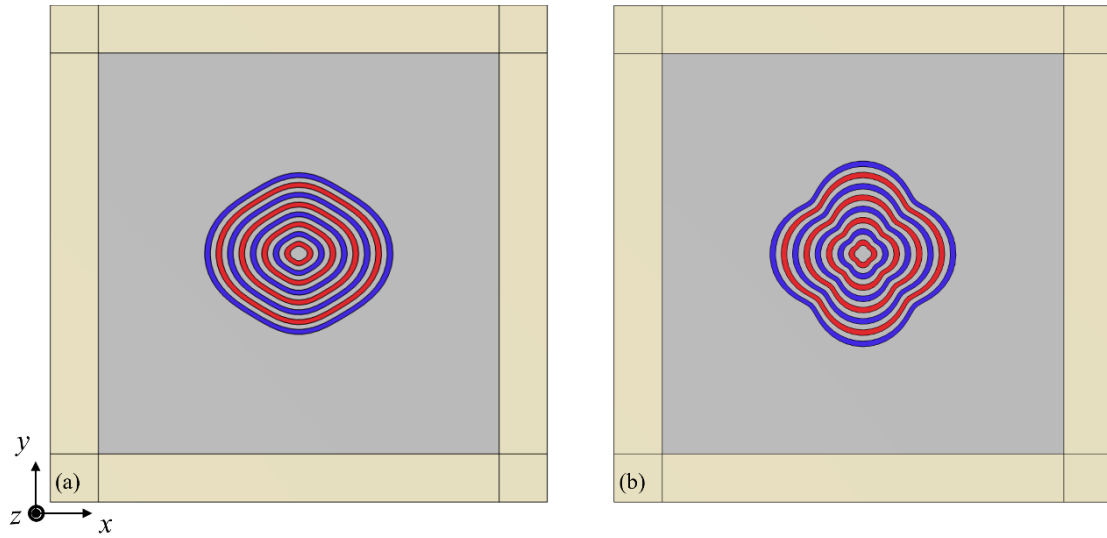


FIGURE 13: THE 3D NUMERICAL MODEL OF THE ANNULAR ARRAY. (A) A0 MODE; (B) S0 MODE

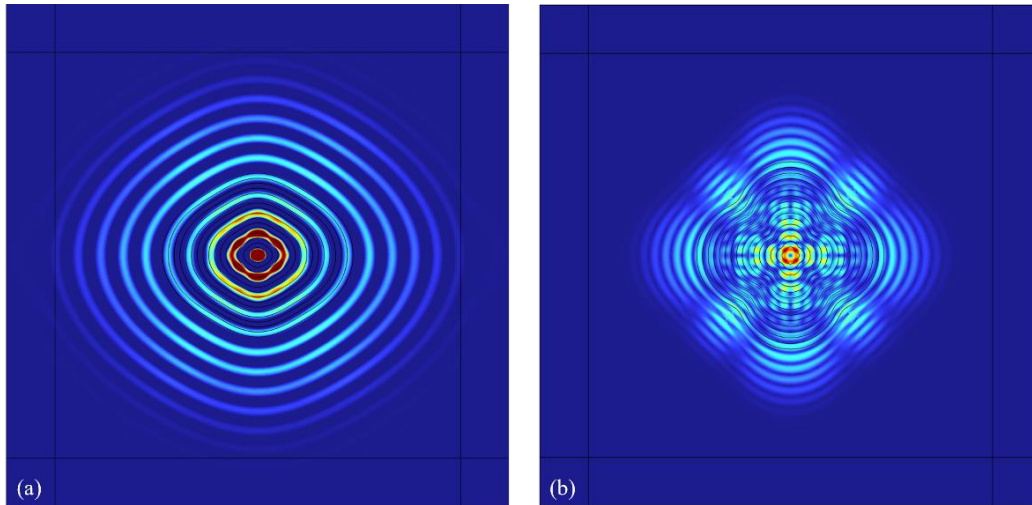


FIGURE 14: THE SURFACE DISPLACEMENT WAVEFIELD OF ANNULAR ARRAY. (A) A0 MODE; (B) S0 MODE

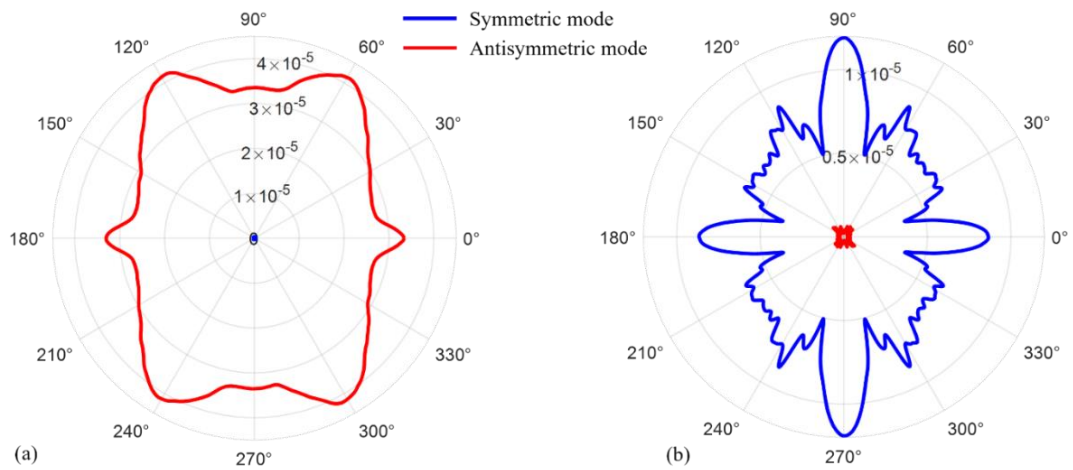


FIGURE 15: THE WAVE DIRECTIONALITY PLOTS IN THE TEMPORAL DOMAIN. (A) A0 MODE; (B) S0 MODE

4. CONCLUSION

This paper presents an innovative method for composite structural health monitoring utilizing dense spray-coating active sensing arrays to generate and receive guided waves. It commences with an analysis of dispersion curves to determine electrode parameters, followed by the development of three-dimensional numerical models with various array patterns. Through meticulous electrode design and wavelength modulations, the approach achieves single-mode generation at comb and IDT type array and omnidirectional single-mode generation at annular array in CFRP composite plate. The numerical results demonstrate the significant potential of the proposed spray-coating sensing arrays system for composite damage detection applications.

ACKNOWLEDGEMENTS

The support from the National Natural Science Foundation of China (contract number 51975357) and the Shanghai Rising-Star Program (contract number 21QA1405100) are thankfully acknowledged.

REFERENCES

- [1] C. Garnier, M.-L. Pastor, F. Eyma, and B. Lorrain, "The detection of aeronautical defects in situ on composite structures using Non Destructive Testing," *Composite Structures*, vol. 93, no. 5, pp. 1328–1336, Apr. 2011, doi: 10/d7nr9d.
- [2] K. B. Katnam, L. F. M. Da Silva, and T. M. Young, "Bonded repair of composite aircraft structures: A review of scientific challenges and opportunities," *Progress in Aerospace Sciences*, vol. 61, pp. 26–42, Aug. 2013, doi: 10/f3tx8m.
- [3] M. A. Drewry and G. A. Georgiou, "A review of NDT techniques for wind turbines," *Insight - Non-Destructive Testing and Condition Monitoring*, vol. 49, no. 3, pp. 137–141, Mar. 2007, doi: 10/d284kp.
- [4] C. C. Ciang, J.-R. Lee, and H.-J. Bang, "Structural health monitoring for a wind turbine system: a review of damage detection methods," *Meas. Sci. Technol.*, vol. 19, no. 12, p. 122001, Dec. 2008, doi: 10/bscrqv.
- [5] R. Raišutis and E. Jasi, "The review of non-destructive testing techniques suitable for inspection of the wind turbine blades," vol. 63, no. 2.
- [6] U. I. K. Galappaththi, A. K. M. De Silva, M. Macdonald, and O. R. Adewale, "Review of inspection and quality control techniques for composite wind turbine blades," *insight*, vol. 54, no. 2, pp. 82–85, Feb. 2012, doi: 10/gtrbtj.
- [7] C. Soutis, "Fibre reinforced composites in aircraft construction," *Progress in Aerospace Sciences*, vol. 41, no. 2, pp. 143–151, Feb. 2005, doi: 10/bh5qrg.
- [8] B. Wang, S. Zhong, T.-L. Lee, K. S. Fancey, and J. Mi, "Non-destructive testing and evaluation of composite materials/structures: A state-of-the-art review," *Advances in Mechanical Engineering*, vol. 12, no. 4, p. 168781402091376, Apr. 2020, doi: 10/gjm3st.
- [9] W. L. Cong, Z. J. Pei, T. W. Deines, and C. Treadwell, "Rotary ultrasonic machining of CFRP using cold air as coolant: feasible regions," *Journal of Reinforced Plastics and Composites*, vol. 30, no. 10, pp. 899–906, May 2011, doi: 10/fpb5mm.
- [10] P. J. Schilling, B. R. Karedla, A. K. Tatiparthi, M. A. Verges, and P. D. Herrington, "X-ray computed microtomography of internal damage in fiber reinforced polymer matrix composites," *Composites Science and Technology*, vol. 65, no. 14, pp. 2071–2078, Nov. 2005, doi: 10.1016/j.compscitech.2005.05.014.
- [11] K. T. Tan, N. Watanabe, and Y. Iwahori, "X-ray radiography and micro-computed tomography examination of damage characteristics in stitched composites subjected to impact loading," *Composites Part B: Engineering*, vol. 42, no. 4, pp. 874–884, Jun. 2011, doi: 10.1016/j.compositesb.2011.01.011.
- [12] P. Liu, R. M. Groves, and R. Benedictus, "3D monitoring of delamination growth in a wind turbine blade composite using optical coherence tomography," *NDT & E International*, vol. 64, pp. 52–58, Jun. 2014, doi: 10.1016/j.ndteint.2014.03.003.
- [13] R. A. Badcock and G. F. Fernando, "An intensity-based optical fibre sensor for fatigue damage detection in advanced fibre-reinforced composites," *Smart Mater. Struct.*, vol. 4, no. 4, pp. 223–230, Dec. 1995, doi: 10.1088/0964-1726/4/4/001.
- [14] P.-M. Lam, K.-T. Lau, H.-Y. Ling, Z. Su, and H.-Y. Tam, "Acousto-ultrasonic sensing for delaminated GFRP composites using an embedded FBG sensor," *Optics and Lasers in Engineering*, vol. 47, no. 10, pp. 1049–1055, Oct. 2009, doi: 10.1016/j.optlaseng.2009.01.010.
- [15] L. Zhiyong, Z. Qinlan, and L. Xiang, "New Magnetic Particle Cassette NDT Intelligent Detection Device," in *2013 Fourth International Conference on Intelligent Systems Design and Engineering Applications*, Zhangjiajie, Hunan Province, China: IEEE, Nov. 2013, pp. 403–406. doi: 10.1109/isdea.2013.496.
- [16] L. Toubal, M. Karama, and B. Lorrain, "Damage evolution and infrared thermography in woven composite laminates under fatigue loading," *International Journal of Fatigue*, vol. 28, no. 12, pp. 1867–1872, Dec. 2006, doi: 10.1016/j.ijfatigue.2006.01.013.
- [17] C. Toscano, C. Meola, M. C. Iorio, and G. M. Carlomagno, "Porosity and Inclusion Detection in CFRP by Infrared Thermography," *Advances in Optical Technologies*, vol. 2012, pp. 1–6, Nov. 2012, doi: 10.1155/2012/765953.
- [18] K. Imielińska, M. Castaings, R. Wojtyra, J. Haras, E. L. Clezio, and B. Hosten, "Air-coupled ultrasonic C-scan technique in impact response testing of carbon fibre and hybrid: glass, carbon and Kevlar/epoxy composites," *Journal of Materials Processing Technology*, vol. 157–158, pp. 513–522, Dec. 2004, doi: 10.1016/j.jmatprotec.2004.07.143.
- [19] M. Cacciola, S. Calcagno, F. C. Morabito, and M. Versaci, "Computational intelligence aspects for defect

- classification in aeronautic composites by using ultrasonic pulses,” *IEEE Trans. Ultrason., Ferroelect., Freq. Contr.*, vol. 55, no. 4, pp. 870–878, Apr. 2008, doi: 10.1109/tuffc.2008.722.
- [20] D. Pagodinas, “Ultrasonic signal processing methods for detection of defects in composite materials”.
- [21] B. Shakibi, F. Honarvar, M. D. C. Moles, J. Caldwell, and A. N. Sinclair, “Resolution enhancement of ultrasonic defect signals for crack sizing,” *NDT & E International*, vol. 52, pp. 37–50, Nov. 2012, doi: 10.1016/j.ndteint.2012.08.003.
- [22] Z. Su, L. Ye, and Y. Lu, “Guided Lamb waves for identification of damage in composite structures: A review,” *Journal of Sound and Vibration*, vol. 295, no. 3–5, pp. 753–780, Aug. 2006, doi: 10/cdnfvj.
- [23] S. Gholizadeh, “A review of non-destructive testing methods of composite materials,” *Procedia Structural Integrity*, vol. 1, pp. 50–57, 2016, doi: 10.1016/j.prostr.2016.02.008.
- [24] S. I. Rokhlin and L. Wang, “Ultrasonic waves in layered anisotropic media: characterization of multidirectional composites,” *International Journal of Solids and Structures*, 2002.
- [25] M. A. Hamstad, “A review: Acoustic emission, a tool for composite-materials studies,” *Experimental Mechanics*, vol. 26, no. 1, pp. 7–13, Mar. 1986, doi: 10.1007/bf02319949.
- [26] Y. Wang, L. Qiu, Y. Luo, R. Ding, and F. Jiang, “A piezoelectric sensor network with shared signal transmission wires for structural health monitoring of aircraft smart skin,” *Mechanical Systems and Signal Processing*, vol. 141, p. 106730, Jul. 2020, doi: 10.1016/j.ymsp.2020.106730.
- [27] P. Li, S. Shan, F. Wen, and L. Cheng, “A fully-coupled dynamic model for the fundamental shear horizontal wave generation in a PZT activated SHM system,” *Mechanical Systems and Signal Processing*, vol. 116, pp. 916–932, Feb. 2019, doi: 10.1016/j.ymsp.2018.07.010.
- [28] M. Mańka, M. Rosiek, A. Martowicz, T. Stepinski, and T. Uhl, “PZT based tunable Interdigital Transducer for Lamb waves based NDT and SHM,” *Mechanical Systems and Signal Processing*, vol. 78, pp. 71–83, Oct. 2016, doi: 10.1016/j.ymsp.2015.12.013.
- [29] Lingyu Yu and V. Giurgiutiu, “Multi-mode Damage Detection Methods with Piezoelectric Wafer Active Sensors,” *Journal of Intelligent Material Systems and Structures*, vol. 20, no. 11, pp. 1329–1341, Jul. 2009, doi: 10.1177/1045389X08096665.
- [30] Wenhao Zhu and J. L. Rose, “Lamb wave generation and reception with time-delay periodic linear arrays: a BEM simulation and experimental study,” *IEEE Trans. Ultrason., Ferroelect., Freq. Contr.*, vol. 46, no. 3, pp. 654–664, May 1999, doi: 10.1109/58.764852.
- [31] J. Jin, S. T. Quek, and Q. Wang, “Analytical Solution of Excitation of Lamb Waves in Plates by Inter-Digital Transducers,” *Proceedings: Mathematical, Physical and Engineering Sciences*, vol. 459, no. 2033, pp. 1117–1134, 2003, doi: 10.1098/rspa.2002.1071.
- [32] E. V. Glushkov, N. V. Glushkova, W. Seemann, and O. V. Kvasha, “Elastic wave excitation in a layer by piezoceramic patch actuators,” *Acoust. Phys.*, vol. 52, no. 4, pp. 398–407, Jul. 2006, doi: 10/bdg8xq.
- [33] Y. Wang, S. Hu, T. Xiong, Y. Huang, and L. Qiu, “Recent progress in aircraft smart skin for structural health monitoring,” *Structural Health Monitoring*, vol. 21, no. 5, pp. 2453–2480, Sep. 2022, doi: 10.1177/14759217211056831.
- [34] Hua Gu and M. L. Wang, “A Monolithic Interdigitated PVDF Transducer for Lamb Wave Inspection,” *Structural Health Monitoring*, vol. 8, no. 2, pp. 137–148, Mar. 2009, doi: 10.1177/1475921708102104.
- [35] B. Ren and C. J. Lissenden, “PVDF Multielement Lamb Wave Sensor for Structural Health Monitoring,” *IEEE Trans. Ultrason., Ferroelect., Freq. Contr.*, vol. 63, no. 1, pp. 178–185, Jan. 2016, doi: 10.1109/tuffc.2015.2496423.
- [36] Y. Zhu, X. Zeng, M. Deng, K. Han, and D. Gao, “Detection of nonlinear Lamb wave using a PVDF comb transducer,” *NDT & E International*, vol. 93, pp. 110–116, Jan. 2018, doi: 10.1016/j.ndteint.2017.09.012.
- [37] V. T. Rathod, G. Raju, L. Udpa, S. Udpa, and Y. Deng, “Multimode guided wave extraction capabilities using embedded thin film sensors in a composite laminated beam,” *Sensors and Actuators A: Physical*, vol. 309, p. 112040, Jul. 2020, doi: 10.1016/j.sna.2020.112040.
- [38] P. D. Wilcox, R. P. Dalton, M. J. S. Lowe, and P. Cawley, “Mode and Transducer Selection for Long Range Lamb Wave Inspection,” *KEM*, vol. 167–168, pp. 152–161, Jun. 1999, doi: 10.4028/www.scientific.net/KEM.167-168.152.
- [39] J. Wang and Y. Shen, “SAFE-DISPERSION: A graphical user interface for modeling guided wave propagation in elastic solids”, doi: 10.1117/12.2582952.
- [40] J. P. Koduru and J. L. Rose, “Transducer arrays for omnidirectional guided wave mode control in plate like structures,” *Smart Mater. Struct.*, vol. 22, no. 1, p. 015010, Jan. 2013, doi: 10.1088/0964-1726/22/1/015010.
- [41] W. Ziping, X. Xiqiang, Q. Lei, W. Jiatao, F. Yue, and T. Maoyuan, “Research on the Progress of Interdigital Transducer (IDT) for Structural Damage Monitoring,” *Journal of Sensors*, vol. 2021, pp. 1–10, Mar. 2021, doi: 10.1155/2021/6630658.
- [42] D. Roy Mahapatra, A. Singhal, and S. Gopalakrishnan, “Numerical analysis of Lamb wave generation in piezoelectric composite IDT,” *IEEE Trans. Ultrason., Ferroelect., Freq. Contr.*, vol. 52, no. 10, pp. 1851–1860, Oct. 2005, doi: 10.1109/tuffc.2005.1561641.